İSTANBUL UNIVERSITY
C E R R A H P A Ş A

A Path Loss Model for Link Budget Analysis of Indoor Visible Light Communications

Farshad Miramirkhani [iD]

Department of Electrical and Electronics Engineering, Işık University, İstanbul, Turkey

ABSTRACT

In the context of beyond 5G indoor communication systems, visible light communications (VLC) has emerged as a viable supplement for existing radio frequency-based systems and as an enabler for high data rate communications. However, the existing indoor VLC systems are limited by detrimental outages caused by fluctuations in the VLC channel-gain because of user mobility. In this study, we proposed a tractable path loss model for indoor VLC that reflects the effect of room size and coating material of surfaces. We performed an extensive advanced ray tracing simulation to obtain the channel impulse responses within a room and presented a path loss model as a function of distance, room size, and coating material through curve fitting. In addition, path loss parameters such as the path loss exponent and the standard deviation of the shadowing component were determined. The simulation results indicate that path loss is a linear function of distance, path loss exponent is a function of room size and coating material, and shadowing follows a log-normal distribution.
Keywords: Path loss, ray tracing, shadowing, visible light communications

Introduction

Visible light communications (VLC) has emerged as a promising green, secure, and interference-free alternative to the existing radio frequency communication technologies for the next generation communication systems [1-3]. Despite increasing literature on visible light and infrared (IR) communications, there is lack of a proper path loss model. This is a serious concern as path loss sheds light on link design and dictates the fundamental limits on the physical layer design of VLC system, that is, transmission power and receiver complexity.

Earlier works on IR channel modeling [4-16] depend on either recursive approaches [4-6] or ray tracing methods [10-12]. In [15, 16], a path loss model inside an airplane cabin was proposed. The path loss parameters (path loss exponent) as well as the shadowing component (standard deviation) were obtained for line-of-sight (LoS) and non-line-of-sight (NLoS) scenarios.

Note that the existing IR channel models cannot be used for VLC in a straightforward manner because there exist significant differences between IR and VLC communications. There have been some efforts [17-24] to address VLC channel modeling; however, the practical considerations such as reflection type and realistic emission pattern of light source were overlooked in previous studies [18-24]. In addition, the authors in [17] assumed a fixed location for receiver; and hence, the effect of mobility was not considered. In [20, 22-24], a constant reflectance value was considered for the coating material of surfaces (that is, wall and floor), which can be justified for IR wavelengths. However, the wavelength-dependent reflectance is indispensable for realistic VLC channel modeling owing to the wideband nature of light emitting diodes (LEDs). Furthermore, in these studies, the path loss model was obtained with a limited number of reflections (up to the order of 2). There are only sporadic works [17, 21], which consider higher order of reflections in the path loss model.

In environments with different reflectivity, it is also shown that the received power is almost proportional to the inverse of the available bandwidth [25]. In other words, in an indoor en-

vironment with high-reflectance coating materials, low path loss is foreseen resulting in high delay spread and low channel bandwidth. By contrast, if the reflectance is low, larger path loss is expected, leading to larger channel bandwidth. Moreover, the VLC channel may vary because of movement, blockage, and shadowing [15, 16].

Therefore, it is obvious that there is a need for the development of a comprehensive channel model that simultaneously considers the effect of user mobility, room size, and coating material of surfaces. In an effort to address this research gap, a closed-form path loss expression as a function of distance, room size, and coating material of surfaces is proposed.

In this study, a site-specific VLC channel modeling approach [17] is adopted to overcome the limitations in earlier works. However, unlike [17] that provides channel impulse responses (CIRs) for some selected points (that is, fixed user) where the room size and coating materials are fixed, in this study, the channel for a mobile user within a room with different dimensions and coating materials is characterized, and it is demonstrated how the channel changes when the user walks within the room. The proposed approach can take into account diffuse, specular, and mixed reflections. It can also handle non-Lambertian light sources. Furthermore, in comparison to conventional ray tracing methods, this approach can consider a larger number of reflections (because of relatively less computing time) for better accuracy.

A comparison of the existing works with adopted approach is summarized in Table 1.

With regard to the literature review, the novelty of this study can be summarized as:

- The VLC channel for a mobile user is characterized using realistic assumptions, such as wavelength-dependent reflection characteristics, mixed diffuse-specular reflections, non-Lambertian light source, and high order of reflections (up to 10).
- A path loss and shadowing model simultaneously considering the effect of user mobility, room size, and coating material of surfaces are developed to investigate changes in the channel when a user walks within the room.

The rest of the paper is organized as follows. In Section 2, the adopted VLC channel modeling approach is summarized. Furthermore, the path loss expression based on the obtained CIRs is proposed where the effect of room size, reflectance of material, and higher order of reflections are explained. In Section 3, the effect of user-mobility is investigated, and the probability distribution function of shadowing is presented. Finally, conclusions are drawn in Section 4.

Channel Modeling Approach

This study adopted the advanced ray-tracing-based channel modeling method in [17]. In this approach, a 3D simulation platform was first created where the geometric specifications of the indoor scenario are determined, and the CAD objects of the users and furniture are integrated into the simulation platform. The reflectance of surfaces (that is, furniture, ceilings, floor, and walls) and the specifications of the transmitter and photodetectors (PDs) are also defined.

Existing Path Loss Models

To evaluate the path loss, most of the works [20, 22-24] focus on scenarios where path loss is obtained with limited reflections (up to the order of 2) specifically assuming zero order reflections (that is, LoS response). The path loss model in these works is expressed as,

$$PL \approx \frac{(m+1)A_r}{2\pi d^2} \cos^m(\alpha)\cos(\beta) \tag{1}$$

where A_r is the receiver area, d is the distance between the light source and receiver, α is the viewing angle of transmitter, β is the incident angle, and m is the order of Lambertian emission. Note that the path loss obtained through (1) is underestimated as the effect of higher order reflections is overlooked. To address this issue, the advanced ray-tracing-based channel modeling method was used to calculate the received optical power and path lengths of each ray from light source to PD. This information was processed in MATLAB® (MathWorks, Natick, Massachusetts, United States), and the CIR was then calculated as

$$h(t) = \sum_{i=1}^{N_r} P_i \, \delta(t - \tau_i) \tag{2}$$

where P_i is the received optical power of the ith ray, T_i, is the traveling time of the ith ray, $\delta(t)$ is the Dirac delta function, and N_r denotes the number of received rays. Channel parameters are calculated on the basis of the obtained CIRs. Channel DC gain is one of the insightful designing parameters as it predicts the averaged received power and is expressed as [17]

$$H_0 = \int_0^\infty h(t)\,dt. \tag{3}$$

The optical path loss can be then obtained as [1]

$$PL = -10\log_{10}\left(\int_0^\infty h(t)\,dt\right). \tag{4}$$

For the time dispersion parameters, the mean excess delay and the root mean square (RMS) delay spread are respectively given by[1]

$$\tau_0 = \frac{\int_0^\infty t\,h(t)\,dt}{\int_0^\infty h(t)\,dt}, \tag{5}$$

$$\tau_{RMS} = \sqrt{\frac{\int_0^\infty (t-\tau_0)^2\,h(t)\,dt}{\int_0^\infty h(t)\,dt}}. \tag{6}$$
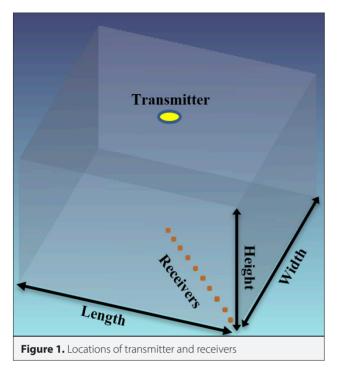
Proposed Path Loss Model

In this section, different sizes for an empty room (that is, small room sizes: 3 m × 3 m–6 m × 6 m and large room sizes: 7 m × 7 m–12 m × 12 m) with a height of 3 m and plaster or glass ceiling/walls and pinewood floor are considered as shown in

Table 1. Comparison of existing path loss models for IR and VLC

		Method	Reflectance Modeling	Number of Reflections	Underlying Assumptions
IR	[14]	Recursive	Fixed Reflectance	2 Order	- Diffuse reflections
					- Furnished room
					- Lambertian source
	[15]	Ray Tracing	Fixed Reflectance	High Order (> 4)	- Diffuse and specular reflections
					- Aircraft cabin
					- Lambertian source
	[16]	Ray Tracing	Fixed Reflectance	High Order (> 4)	- Diffuse and specular reflections
					- Aircraft cabin
					- Lambertian source
VLC	[20]	Recursive	Fixed Reflectance	1 Order	- Diffuse reflections
					- Empty Room
					- Lambertian source
	[21]	Ray Tracing	Wavelength Dependent	High Order (> 4)	- Diffuse reflections
					- Empty room with the presence of a cylindrical object to model a user
					- Lambertian source
	[22]	Recursive	Fixed Reflectance	1 Order	- Diffuse reflections
					- Furnished room
					- Lambertian source
	[23]	Recursive	Fixed Reflectance	2 Order	- Diffuse reflections
					- Furnished room
					- Realistic measured source
	[24]	Recursive	Fixed Reflectance	1 Order	- Diffuse and specular reflections
					- Empty Room
					- Lambertian source
Adopted Approach	[17]	Ray Tracing	Wavelength Dependent	High Order (> 10)	- Diffuse, specular and mixed reflections
					- Furnished room and realistic human models
					- Realistic measured source

IR: infrared; VLC: visible light communications

Figure 1. Two ultimate cases of spectral reflectance value are assumed where plaster and glass have the highest and lowest reflectance values, respectively [17]. The wavelength-dependent reflectance of coating material for each surface is defined using the "table coating method" in adopted advanced ray tracing approach. The transmitter is placed at the center of the ceiling. This is a commercial LED (Cree® CR6-800L) with a half view angle of 40º. The optical power of luminaire was normalized to 1 W by which the channel DC gain is associated with the averaged received power [17]. Without loss of generality and because of the symmetric shape of the room, 10 PDs on the diagonal of the room are considered, that is, stretches from the

Figure 1. Locations of transmitter and receivers

Figure 2. a, b. Channel impulse responses for detectors placed at (a) the center and (b) the corner of the room

corner to the middle of the room. The field of view (FOV) and the detector area size are 85^0 and 1 cm², respectively.

According to the obtained CIRs, the path loss for different room sizes with plaster (or glass) ceiling/walls is calculated. Through curve fitting, the path loss is obtained as,

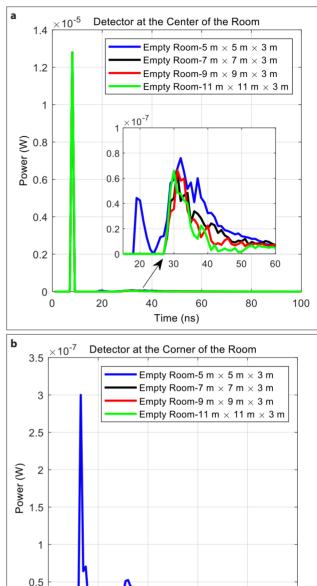$$PL = -10\log_{10}\left(\frac{a}{d^n}\right) \qquad (7)$$

where d is the distance between light source and PD, and the path loss exponent n is given by
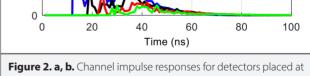
$$n = \begin{cases} 3.6 \sim 4.5 & \text{small room size-plaster wall/ceiling} \\ 5 \sim 5.4 & \text{small room size-glass wall/ceiling} \\ 4.8 & \text{large room size-plaster wall/ceiling} \\ 5.4 & \text{large room size-glass wall/ceiling} \end{cases} \qquad (8)$$

The related coefficient a is presented in Table 2.

It is observed from Table 2 that the path loss exponent increases as the room size increases. Therefore, the effect of higher order reflections is less pronounced as the room size increases. It is also observed that there is no noticeable change in the path loss exponent for the room sizes larger than 7 m × 7 m and 5 m × 5 m for the plaster and glass coatings, respectively. The simulation results further reveal that the path loss exponent in the room with glass wall/ceiling is larger than the one with plaster coating, and it fast approaches a fixed value.

As a benchmark, the path loss components for LoS response was also obtained (Table 3). It is observed from Table 3 that the path loss exponent is independent of the coating material and the room size. Therefore, the effect of reflections from the surfaces are not considered in the LoS response.

In addition, the effect of room size on the channel parameters and CIR is investigated. As two extreme cases, the receiver is located at the corner and the center of the room with plaster ceiling/walls. The CIRs are presented in Figure 2, and the channel parameters are summarized in Table 4. The simulation results revealed that the multipath effect is more pronounced when the detector is moved to the corner of the room. Moreover, it is observed that the amplitude of the channel for the detector placed at the center of the room is larger than that when the detector placed in the corner of the room.
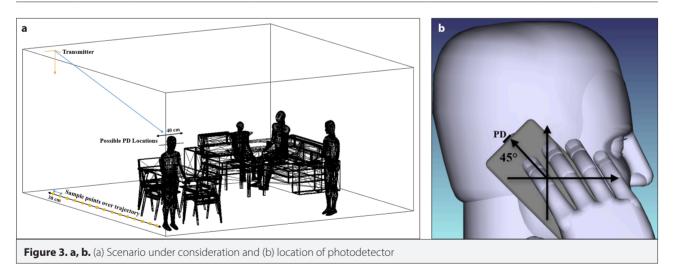
Table 2. Channel coefficients for different room sizes considering higher order reflections

	Length (m) × Width (m)									
	3×3	**4×4**	**5×5**	**6×6**	**7×7**	**8×8**	**9×9**	**10×10**	**11×11**	**12×12**
Plaster ceiling/Walls										
a	2.40e-4	2.78e-4	3.39e-4	4.22e-4	5.26e-4	5.34e-4	5.20e-4	5.19e-4	5.27e-4	5.21e-4
n	3.6	3.9	4.2	4.5	4.8	4.8	4.8	4.8	4.8	4.8
Glass ceiling/Walls										
a	5.82e-4	6.85e-4	8.06e-4	7.97e-4	7.94e-4	8.12e-4	7.96e-4	7.95e-4	8.15e-4	8.05e-4
n	5	5.2	5.4	5.4	5.4	5.4	5.4	5.4	5.4	5.4

Table 3. Channel coefficients for different room sizes considering LoS

	Length (m) × Width (m)									
	3×3	**4×4**	**5×5**	**6×6**	**7×7**	**8×8**	**9×9**	**10×10**	**11×11**	**12×12**
a	3.85e-4	3.98e-4	4.01e-4	3.97e-4	3.95e-4	4.05e-4	3.97e-4	3.96e-4	4.06e-4	4.01e-4
n	5.4	5.4	5.4	5.4	5.4	5.4	5.4	5.4	5.4	5.4

LoS: line of sight

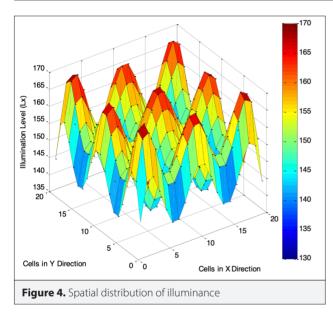**Figure 3. a, b.** (a) Scenario under consideration and (b) location of photodetector
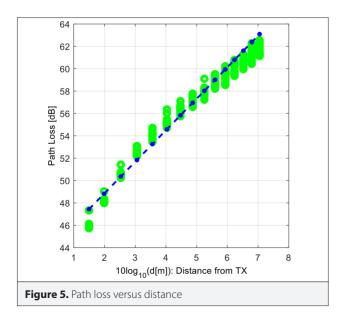
Shadowing Model

In this section, the shadowing that reflects the effect of receiver mobility in the path loss model is investigated. A living room as one of the reference scenarios endorsed by IEEE 802.15.7r1, with a size of 6 m × 6 m × 3 m is considered (Figure 3), where the ceiling/walls and floor are coated with plaster and pinewood, respectively. The coating material of the table/chairs, sofa, and coffee table are respectively defined as pinewood, cotton, and glass. The heads and hands of the users are modeled as an absorbing coating, whereas black gloss shoes and cotton clothes are defined. Nine equally spacing commercial luminaires (Cree® CR6-800L) are placed on the ceiling with half viewing angle of 40º. The optical power of each luminaire was
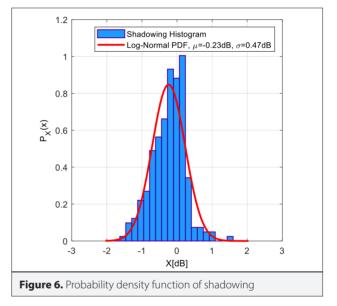
11 W by which an average illumination of 153 lux, that is, the illumination requirement for home [26] is satisfied (Figure 4).

Without loss of generality, a sample trajectory next to the wall and furniture is considered (Figure 3a) to capture the effect of reflected rays in the shadowing model. Fifteen sample locations with an equal spacing of 30 cm over this trajectory were considered to ensure a continuous movement of the mobile user. The user holds a cell phone in his/her hand next to his/her ear, and the detector is placed on the phone (Figure 3b). For PD, 18 possible locations on the right- and left-hand sides of the user's ear, that is, 9 locations on each side, are assumed to model the possible movement of the user's head (Figure 3a).

Table 4. Channel parameters for different room sizes where the detector is placed at the center and corner of the room

		$T_{RMS}^{(ns)}$	H_0	PL (dB)
Center of the Room	5 m × 5 m	8.36	$1.39×10^{-5}$	48.54
	7 m × 7 m	7.98	$1.35×10^{-5}$	48.67
	9 m × 9 m	7.65	$1.34×10^{-5}$	48.70
	11 m × 11 m	7.07	$1.33×10^{-5}$	48.74
Corner of the Room	5 m × 5 m	12.78	$1.44×10^{-6}$	58.41
	7 m × 7 m	12.81	$5.87×10^{-7}$	62.31
	9 m × 9 m	14.25	$3.56×10^{-7}$	64.48
	11 m × 11 m	14.61	$2.17×10^{-7}$	66.63

Figure 4. Spatial distribution of illuminance

Figure 6. Probability density function of shadowing

Figure 5. Path loss versus distance

The PD locations are assumed with an equal spacing of 2.5 cm; hence, a maximum movement of 40 cm for the user's head can be modeled. The detectors are placed at a height of 1.8 m with 45° rotation. The FOV and the detector area size were 85° and 1 cm², respectively. On the basis of the obtained CIRs for 18 receivers in each location of moving human, the path loss model can be obtained as,

$$PL = -10\log_{10}\left(\frac{P_R(d)}{P_T}\right) = -10\log_{10}\left(\frac{a}{d^n}\right) + X_{\mu,\sigma} \tag{9}$$

where α is $9.60 × 10^{-5}$, *n* is 3.9 (Figure 5), and $X_{\mu,\sigma}$ follows a log normal distribution (Figure 6) with mean *μ* and standard deviation *σ* that reflects the shadowing effect. The mean and standard deviation are 0.23 dB and 0.47 dB, respectively. It can be observed from Figure 5 that path loss is a linear function of distance between transmitter and receiver, and the path loss exponent is in the range of 3.6~4.5 (that is, small room size with plaster walls/ceiling) as is expected from (8).

Conclusion

In this study, a closed form path loss expression to integrate the effect of room size, coating material, and higher order of reflections was proposed. It was observed that the path loss exponent was in the range of 3.6–5.4. The simulation results also revealed that the effect of higher order reflections was less pronounced as the room size increased. Moreover, there was no noticeable change in the path loss exponent for the room sizes larger than 7 m × 7 m and 5 m × 5 m for the plaster and glass coatings, respectively. Furthermore, the path loss for a mobile user walking in a realistic indoor environment was modeled. It was shown that the path loss was a linear function of distance between transmitter and receiver and the shadowing component due to the movement of the detector is a log-normal distributed random variable.

Peer-review: Externally peer-reviewed.

Conflict of Interest: The authors have no conflicts of interest to declare.

Financial Disclosure: The authors declared that this study has received no financial support.

References

1. F. Miramirkhani, and M. Uysal, "Channel modelling for indoor visible light communications", Philos. T. R. Soc. A, Special Issue on The Cross-Disciplinary Challenges towards Mobile Optical Wireless Networks, vol. 378, no. 2169, pp. 1-35, Mar. 2020. [Crossref]

2. M. Uysal, F. Miramirkhani, O. Narmanlioglu, T. Baykas, and E. Panayirci, "IEEE 802.15.7r1 reference channel models for visible light communications", IEEE Commun. Mag., vol. 55, no. 1, pp. 212-217, Jan. 2017. [Crossref]

3. M. Uysal, C. Capsoni, Z. Ghassemlooy, A. Boucouvalas, and E. Udvary, "Optical wireless communications: An emerging technology", Springer, Berlin, Germany, 2016. [Crossref]

4. F. R. Gfeller, and U. Bapst, "Wireless in-house data communication via diffuse infrared radiation", Proc. IEEE, vol. 67, no. 11, pp. 1474-1486, Nov. 1979. [Crossref]

5. J. R. Barry, J. M. Kahn, W. J. Krause, E. A. Lee, and D. G. Messerschmitt, "Simulation of multipath impulse response for wireless optical channels", IEEE J. Sel. Areas Commun., vol. 11, no. 3, pp. 367-379, Apr. 1993. [Crossref]

6. J. B. Carruthers, and P. Kannan, "Iterative site-based modeling for wireless infrared channels", IEEE Trans. Antennas Propag., vol. 50, no. 5, pp. 759-765, May 2002. [Crossref]

7. J. B. Carruthers, and J. M. Kahn, "Modelling of non-directed wireless infrared channels", IEEE Trans. Commun., vol. 45, no. 10, pp. 1260-1268, Oct. 1997. [Crossref]

8. R. Perez-Jimenez, J. Berges, and M. J. Betancor, "Statistical model for the impulse response on infrared indoor diffuse channels", IEEE Electron. Lett., vol. 33, no. 15, pp. 1298-1300, Jul. 1997. [Crossref]

9. R. Perez-Jimenez, V. M. Melian, and M. J. Betancor, "Analysis of multipath impulse response of diffuse and quasi-diffuse optical links for IR-WLAN", in Proceedings of the Fourteenth Annual Joint Conference of the IEEE Computer and Communications Societies, Boston, MA, 1995, pp. 924-930.

10. F. J. Lopez-Hernandez, R. Perez-Jimeniz, and A. Santamaria, "Monte Carlo calculation of impulse response on diffuse IR wireless in-door channels", IEEE Electron. Lett., vol. 34, no. 12, pp. 1260-1262, Jun. 1998. [Crossref]

11. F. J. Lopez-Hernandez, R. Perez-Jimenez, and A. Santamaria, "Modified Monte Carlo scheme for high-efficiency simulation of the impulse response on diffuse IR wireless indoor channels", IEEE Electron. Lett., vol. 34, no. 19, pp. 1819-1820, Sept. 1998. [Crossref]

12. F. J. Lopez-Hernandez, R. Perez-Jimenez, and A. Santamaria, "Ray tracing algorithms for fast calculation of the channel impulse response on diffuse IR wireless indoor channels", Opt. Eng., vol. 39, no. 10, pp. 2775-2780, Oct. 2000. [Crossref]

13. M. I. Sakib Chowdhury, W. Zhang, and M. Kavehrad, "Combined deterministic and modified Monte Carlo method for calculating impulse responses of indoor optical wireless channels", J. Lightwave Technol., vol. 32, no. 18, pp. 3132-3148, Sept. 2014. [Crossref]

14. A. G. Al-Ghamdi, and J. M. Elmirghani, "Performance comparison of LSMS and conventional diffuse and hybrid optical wireless techniques in a real indoor environment", IEE Proc. Optoelectron., vol. 152, no. 4, pp. 230-238, Aug. 2005. [Crossref]

15. S. Dimitrov, R. Mesleh, H. Haas, M. Cappitelli, M. Olbert, and E. Bassow, "Path loss simulation of an infrared optical wireless system for aircrafts", in IEEE Global Telecommunications Conference, Honolulu, HI, 2009, pp. 1-6. [Crossref]

16. S. Dimitrov, R. Mesleh, H. Haas, M. Cappitelli, M. Olbert, and E. Bassow, "On the SIR of a cellular infrared optical wireless system for an aircraft", IEEE J. Sel. Areas Commun., vol. 27, no. 9, pp. 1623-1638, Dec. 2009. [Crossref]

17. F. Miramirkhani, and M. Uysal, "Channel modeling and characterization for visible light communications", IEEE Photon. J., vol. 7, no. 6, pp. 1-16, Nov. 2015. [Crossref]

18. P. H. Pathak, X. Feng, P. Hu, and P. Mohapatra, "Visible light communication, networking, and sensing: A survey, potential and challenges", IEEE Commun. Surv. Tutorials, vol. 17, no. 4, pp. 2047-2077, Sept. 2015. [Crossref]

19. B. Hussain, X. Li, F. Che, C. P. Yue, and L. Wu, "Visible light communication system design and link budget analysis", J. Lightwave Technol., vol. 33, no. 24, pp. 5201-5209, Nov. 2015. [Crossref]

20. T. Komine, S. Haruyama, and M. Nakagawa, "A study of shadowing on indoor visible-light wireless communication utilizing plural white LED lightings", Wireless Pers. Commun., vol. 34, no. 1-2, pp. 211-225, Jul. 2005. [Crossref]

21. Y. Xiang, M. Zhang, M. Kavehrad, M. S. Chowdhury, M. Liu, J. Wu, and X. Tang, "Human shadowing effect on indoor visible light communications channel characteristics", Opt. Eng., vol. 53, no. 8, pp. 086113-086113, Aug. 2014. [Crossref]

22. P. Chvojka, S. Zvanovec, P. A. Haigh, and Z. Ghassemlooy, "Channel characteristics of visible light communications within dynamic indoor environment", J. Lightwave Technol., vol. 33, no. 9, pp. 1719-1725, Feb. 2015. [Crossref]

23. A. T. Hussein, and J. M. Elmirghani, "Performance evaluation of multi-gigabit indoor visible light communication system", in 20th IEEE European Conference on Networks and Optical Communications, London, 2015, pp. 1-6. [Crossref]

24. P. F. Mmbaga, J. Thompson, and H. Haas, "Performance analysis of indoor diffuse VLC MIMO channels using angular diversity detectors," J. Lightwave Technol., vol. 34, no. 4, pp. 1254-1266, Nov. 2016. [Crossref]

25. V. Pohl, V. Jungnickel, and C. von Helmolt, "A channel model for wireless infrared communication", in 11th IEEE International Symposium on Personal Indoor and Mobile Radio Communications, London, 2000, pp. 297-303.

26. Lighting of indoor workplaces, Standard ISO 8995:2002 CIE S 008/E-2001, 2001.

Farshad Miramirkhani received his B.Sc. and M.Sc. degrees in Electrical and Electronics and Communication Engineering from the University of Isfahan, Isfahan, Iran, in 2011 and 2014, respectively. He received his PhD in Electrical and Electronics Engineering from Ozyegin University, Istanbul, Turkey in 2018. Currently, he is an assistant professor in the Department of Electrical and Electronics Engineering, Isik University. He serves as a member of the Telecommunications Advisory Board of Cambridge Scholars Publishing, academic editor of IntechOpen, and editorial board member of Wireless Communications for Frontiers in Communications and Networks. He has also contributed to the standardization works of IEEE 802.15.13 (Short Range Optical Wireless Communications) and IEEE 802.11bb (Light Communications for Wireless Local Area Networking). The LiFi channels developed by Dr. Miramirkhani were selected as the LiFi Reference Channel Models by the IEEE 802.15.13 and IEEE 802.11bb task groups. His current research interests include optical wireless communications, indoor visible light communications, underwater visible light communications, vehicular visible light communications, and channel modeling.